Iodine binding to Humic Acid

Bowley H.E.[1,2], Young S.D.[1,*], Ander E.L.[2], Crout N.M.J.[1], Watts M.J.[2] & Bailey E.H.[1]

[1] University of Nottingham, School of Biosciences, Sutton Bonington Campus, Loughborough, Leics, LE12 5RD UK.

[2] Inorganic Geochemistry, Centre for Environmental Geochemistry, British Geological Survey, Keyworth, Nottingham, NG12 5GG, UK.

*Corresponding Author

1 Abstract

The rate of reactions between humic acid (HA) and iodide (I^-) and iodate (IO_3^-) have been investigated in suspensions spiked with ^{129}I at concentrations of 22, 44 and 88 µg L^{-1} and stored at 10°C. Changes in the speciation of $^{129}I^-$, $^{129}IO_3^-$ and mixed ($^{129}I^-$+$^{129}IO_3^-$) spikes were monitored over 77 days using liquid chromatography inductively coupled plasma mass spectrometry (LC-ICP-MS). In suspensions spiked with $^{129}I^-$ 25% of the added I^- was transformed into organic iodine (Org-^{129}I) within 77 days and there was no evidence of $^{129}IO_3^-$ formation. By contrast, rapid loss of $^{129}IO_3^-$ and increase in both $^{129}I^-$ and Org-^{129}I was observed in $^{129}IO_3^-$-spiked suspensions. However, the rate of Org-^{129}I production was greater in mixed systems compared to $^{129}IO_3^-$-spiked suspensions with the same total ^{129}I concentration, possibly indicating IO_3^-—I^- redox coupling. Size exclusion chromatography (SEC) demonstrated that Org-^{129}I was present in both high and low molecular weight fractions of the HA although a slight preference to bond with the lower molecular weight fractions was observed indicating that, after 77 days, the spiked isotope had not fully mixed with the native ^{127}I pool. Iodine transformations were modelled using first order rate equations and fitted rate coefficients determined. However, extrapolation of the model to 250 days indicated that a pseudo-steady state would be attained after ~ 200 days but that the proportion of ^{129}I incorporated into HA was less than that of ^{127}I indicating the presence of a recalcitrant pool of ^{127}I that was unavailable for isotopic mixing.

Keywords: Humic acid; iodine; kinetics; speciation; iodine-129; soil.

2 Introduction

Iodine is an essential micro-nutrient for all mammals, with a recommended daily dietary intake of

100-150 μg d^{-1} for humans (Johnson, 2003). Iodine deficiency diseases (IDDs) are a global health problem, estimated to affect up to one third of the world's population (WHO, 2004). They are a significant social and economic stress on developing countries and an area of concern for developed countries (WHO 2008). Mechanisms that control the transfer of iodine from the terrestrial environment to the food chain are a poorly understood component of global iodine cycles (Johnson 2003a).

Soil iodine concentrations in the UK are typically within the range 0.5 – 100 mg kg^{-1} (Whitehead, 1984, Johnson, 2003b). Seawater is considered to be the largest source of iodine to the terrestrial biosphere (Muramatsu and Wedepohl, 1998, Fuge and Johnson, 1986) therefore higher soil concentrations tend to occur in coastal areas. High soil iodine concentrations are also often associated with high organic matter content, with humus the primary reservoir of soil iodine (Dai et al., 2009, Smyth and Johnson, 2011, Xu et al., 2011b). In general, a larger soil iodine concentration generally results in greater iodine uptake by plants (Weng et al., 2008, Dai et al., 2006), however iodine associated with organic matter appears to be relatively unavailable for plant uptake (Keppler et al., 2003, Xu et al., 2011b, Xu et al., 2012).

Humic acid (HA) is the colloidal fraction of humus, containing both aliphatic and aromatic moieties, depending on the degree of humification and the original vegetation source of the organic matter. Its large surface area and significant presence in soil organic matter mean that it is highly influential in determining soil iodine dynamics (Xu et al., 2011b, Yamada et al., 2002, Francois, 1987, Hansen et al., 2011, Allard, 2006). Although the composition of HA varies between soils, the functional groups present are similar and therefore understanding iodine interactions with HA contributes significantly to understanding its dynamics in soil (Schlegel et al., 2006, Warner et al., 2000, Saunders et al., 2012). A few authors have investigated reactions between HA and iodine (e.g. Christiansen and Carlsen, 1991, Reiller et al., 2006, Choung et al., 2013) but the majority of studies involve other reaction components, often in complex media such as aerosols; the rate of reaction between I and HA has generally not been explicitly considered. Iodination of HA is thought to occur mainly via reduction of IO_3^- to produce reactive intermediate species, such as I_2 or HOI, followed by electrophilic substitution reactions with electron donor groups on the HA (Francois 1987). Whitehead (1974) identified weakly acidic phenolic and amino acid groups as the most likely reaction sites. Christiansen and Carlsen (1991) concluded that HA reacted with a transient iodine species resulting from reaction between I^-, peroxidase enzymes and hydrogen peroxide over 20 minutes, although they were unable to determine whether the transient species was an enzyme-iodine complex or HOI/I_2 produced by action of the peroxidase on I^-. They suggested three possible

types of sites in the HA were available for reaction: primary sites where I was weakly bonded, secondary sites susceptible to nucleophilic iodide-iodide substitution and tertiary electrophilic sites. They also observed that iodine appeared to be uniformly distributed across all molecular size fractions. Schlegel et al. (2006) used Extended X-ray Absorption Fine Structure (EXAFS) to investigate naturally iodinated marine-derived humic substances with 10% iodine by weight and concluded that iodine was covalently bonded, primarily to aromatic rings, but probably present as more than one type of organic species. Preferential bonding of iodine to polycyclic aromatic moities in black carbon was also demonstrated by Choung et al. (2013).

The objectives of this work were to (i) measure and model the dynamics of the reaction between IO_3^- and I^- and HA (ii) establish whether HA contains a recalcitrant (unreactive) pool of iodine and (iii) investigate whether iodine exhibits preferential association with high or low molecular weight moieties in HA. This directly addresses our currently poor understanding of the interaction of iodine with soil organic matter.

3 Materials and methods

3.1 Preparation and characterisation of humic acid solutions

Humic acid (HA) was extracted from a coniferous plantation soil, Leicestershire, UK (52° 42' N, 1° 14' W; 195 m) by shaking for twelve hours with 0.1 M NaOH, followed by centrifugation (10,000 g, 15 min) and acidification to pH 2 of the supernatant, using concentrated HCl. Humic and fulvic fractions were separated by centrifugation and the HA was purified using dialysis against 1 %v/v HCl and HF then deionised water; the resultant HA was then freeze dried and finely ground (Marshall et al., 1995). A portion of dried, ground HA was dissolved in 0.016 M NaOH and adjusted to pH 7.0 using NaOH to give a final concentration of 7.18 mg HA mL^{-1}. A neutral pH value was chosen to be close to typical arable soil conditions and avoid volatilization of I_2. Dissolved organic carbon in the HA solution was determined using a Shimadzu TOC-VCPH analyser. Each sample was acidified to pH 2-3 using HCl to remove inorganic carbon, before the remaining (organic) carbon was detected as CO_2 by non-dispersive infrared detection after heating the sample to 720 °C with a platinum-coated alumina catalyst. Samples were quantified against standards of 2.125 g L^{-1} potassium hydrogen phthalate (C concentration = 1000 mg L^{-1}), diluted to appropriate concentrations with Milli-Q water (18.2 MΩ cm). Total iodine concentration in the HA suspension was measured by ICP-MS (Thermo-Fisher Scientific X-Series^{II}) using internal detector cross-calibration with Rh and Re (10 µg L^{-1}) as internal standards. Stock standards for ^{127}I were prepared at iodine concentrations of 1000 mg L^{-1} from oven-dried KI and KIO_3, and stored at 4 °C in 1 % tetra methyl ammonium hydroxide (TMAH).

Iodine-129 was obtained as a solution of sodium iodide ($^{129}I^-$) from the American National Institute of Standards (NIST, Gaithersburg, Maryland, USA; CRM 4949C, 0.004 mol L^{-1} $Na^{129}I$, 3451 Bq mL^{-1}). Iodate-129 ($^{129}IO_3^-$) was prepared by oxidation of $^{129}I^-$ with sodium chlorite using a method adapted from Yntema and Fleming (1939). Successful oxidation to IO_3^- was confirmed by ICP-MS with in-line chromatographic separation using HPLC (Dionex, ICS-3000) operated in isocratic mode with an anion exchange column (Hamilton PRP-X100; 250 x 4.6 mm, 5 μm particle size). The mobile phase (1.3 mL min^{-1}) was 60 mmol L^{-1} NH_4NO_3, 1 x 10^{-5} mmol L^{-1} Na_2-EDTA, 2% methanol; pH was adjusted to 9.5 with TMAH.

Triplicate aliquots of HA solution (pH 7) were spiked with $^{129}I^-$ and/or $^{129}IO_3^-$ on 8 occasions to give incubation times of 26, 79, 155, 328, 596, 992, 1404 and 1855 hr. Samples were stored in the dark at 10 °C, the average annual soil temperature measured at Armagh Observatory, Northern Ireland (Garcia-Suarez and Butler, 2006). Final concentrations of spiked iodine were 22.1 , 44.1 and 88.2 μg L^{-1} (Table 1). The CRM 4949C contained ^{127}I equivalent to 12 % of the ^{129}I concentration; this was accounted for as described in Electronic Annex A so that, for simplicity, all iodine added in the spike (^{129}I + ^{127}I) is referred to as ^{129}I and native iodine is described as ^{127}I.

3.2 Iodine speciation

Iodine species were separated using HPLC (Dionex, ICS-3000), with a Superose 12 10/300 GL size exclusion chromatography (SEC) column (GE Healthcare), linked to ICP-MS. A sample injection volume of 25 μl and isocratic elution with 0.1 M Tris (Tris(hydroxymethyl)aminomethane) adjusted to pH 8.8 using 50 % Trace Analysis Grade (TAG) HNO_3 at a flowrate of 1 mL min^{-1} was used. The HPLC was controlled using Chromeleon software (Dionex, version 6.80SR12) and sample processing was undertaken using Plasmalab software. Working standards of $^{127}I^-$ and $^{127}IO_3^-$, at iodine concentrations of 0 – 100 μg L^{-1}, were used. Species-specific quantification was carried out with standards of $^{127}I^-$, $^{127}IO_3^-$, $^{129}I^-$ and $^{129}IO_3^-$ prepared in Milli-Q water and mean, isotope-specific, sensitivity values (signal (integrated CPS) per ppb) calculated from iodide and iodate standards were used to quantify HA-bonded iodine (HA-I); drift correction was applied by analysis of repeated standards through the experimental run. Limits of detection were 0.047 μg L^{-1} for ^{127}I and 0.014 μg L^{-1} for ^{129}I. Humic acid controls, spiked with Milli-Q water, were analysed alongside ^{129}I-spiked samples to determine the equilibrium speciation of native ^{127}I.

A correction factor for ^{129}Xe was determined for each run and applied to all ^{129}I results, according to Equation 1:

$$^{129}\mathrm{S} = {}^{129}\mathrm{S}_{\mathrm{meas}} - (k \times {}^{131}\mathrm{S}_{\mathrm{meas}}) \quad (1)$$

where ^{129}S = corrected signal (CPS) for ^{129}I; $^{129}S_{meas}$ = measured signal at m/z = 129; *k* = a factor determined by iteration for each run (typically 1.08) to give an average ^{129}S baseline of zero; $^{131}S_{meas}$ = measured signal for ^{131}Xe. Matrix matching and standard addition were used to calculate mean sensitivity for all samples in each run, from which concentrations of ^{129}I and ^{127}I in each peak were quantified.

3.3 Modelling

Iodine-129 transformations were represented as simultaneous ordinary differential equations (Fig. 1):

$$\frac{d[IO_3^-]}{dt} = -(k_1+k_4)[IO_3^-] + k_5[\text{Org-I}] \quad (2)$$

$$\frac{d[I^-]}{dt} = -k_3[I^-] + k_1[IO_3^-] + k_2[\text{Org-I}] \quad (3)$$

$$\frac{d[\text{Org-I}]}{dt} = -(k_2+k_5)[\text{Org-I}] + k_4[IO_3^-] + k_3[I^-] \quad (4)$$

Where k_1, k_2, k_3, k_4 and k_5 are unknown rate coefficients (hr^1) estimated by fitting the model to the observed concentrations of $^{129}IO_3^-$, $^{129}I^-$ and Org-^{129}I.

The differential equations were solved using 4th order Runge-Kutta and fitting was performed using a Marquardt procedure (Press et al, 1986) implemented in OpenModel (Tarsitano et al 2011, http://openmodel.info/) to minimize the residual sum of squares (RSS) between modelled and observed values over all the time points and different spike combinations. Alternative model structures were considered, the arrangement described (and shown schematically in Fig. 1) provided the best fit to the data.

4 Results and discussion

4.1 Iodine dynamics

Measured characteristics of the HA are given in Table 2. Concentrations of ^{127}I species represent iodine in equilibrium with HA suspensions with median values of 98.0 µg L^{-1} of Org-^{127}I and 15.1 µg L^{-1} $^{127}I^-$; iodate ($^{127}IO_3^-$) was not detected. The C:I mole ratio in the HA was 396,000.

Figure 2 shows the change in speciation of spiked ^{129}I over time; model fits to the data are discussed in a later section. In suspensions spiked with I^- only (Table 1: I_{22}, I_{44} and I_{88}) a gradual decrease in $^{129}I^-$ concentrations was observed over time with a concomitant increase in Org-^{129}I. By the final time point (1855 hr) ~25% of added $^{129}I^-$ had been transformed to Org-^{129}I irrespective of initial spike

concentration. No generation of $^{129}IO_3^-$ was observed. Suspensions spiked with $^{129}IO_3^-$ (Table 1: IO_{22}, IO_{44} and IO_{88}) showed rapid initial loss of $^{129}IO_3^-$ with associated increases in both $^{129}I^-$ and Org-^{129}I. Concentrations of $^{129}I^-$ were always greater than Org-^{129}I. By the end of the experiment (1855 hr) concentrations of $^{129}IO_3^-$ in each system were < 5% of the initial concentrations and Org-^{129}I accounted for ~40% of the added iodine, again irrespective of initial spike concentration. In mixed systems (Table 1; Mix_{22}, Mix_{44} and Mix_{88}), where equal concentrations of $^{129}I^-$ and $^{129}IO_3^-$ were added, results were similar to those observed when $^{129}IO_3^-$ alone was added (Figure 2). Concentrations of $^{129}IO_3^-$ decreased rapidly with both $^{129}I^-$ and Org-^{129}I increasing over time. Again no concentration-dependence was observed, with similar proportions of $^{129}I^-$ and Org-^{129}I observed regardless of spike concentration.

Humic acid has been reported to both reduce IO_3^- and oxidise I^- in soils (Yamaguchi et al., 2010), however oxidation of I^- by organic matter to form IO_3^- is expected to be much slower than reduction of IO_3^- to I^- (Schlegel et al., 2006) unless Fe^{III} and Mn^{IV} oxides are present which may catalyse the oxidation of I^- (Gallard et al., 2009, Allard et al., 2009, Fox et al., 2009). This difference in rate (between I^- and IO_3^-), in the absence of metal oxides, was confirmed by the absence of $^{129}IO_3^-$ in $^{129}I^-$ spiked systems, in contrast to the rapid production of $^{129}I^-$ in HA solutions spiked with $^{129}IO_3^-$. Shetaya et al. (2012), selected soils with a range of pH values and concentrations of Fe/Mn oxides and organic matter for incubation with $^{129}I^-$ or $^{129}IO_3^-$ at 10°C and 20°C. In contrast to the current study, and that of Choung et al. (2013), they found that conversion of added $^{129}I^-$ to (humic-bound) Org-^{129}I ($t_{½}$ = 0.38 – 45 hr) was faster than conversion of $^{129}IO_3^-$ to Org-^{129}I ($t_{½}$ = 9.0 -412 hr). Comparison of these half-life values for whole soil with the data comparing iodide and iodate in Fig. 2 may indicate the importance of metal oxides in soils in rapidly adsorbing IO_3^-, and thereby slowing its transformation into Org-I, or possibly enabling oxidation of I^- to an intermediate species capable of reacting with humus. Additionally the large overall differences in reaction rates seen between soils and HA may reflect enzyme activity in soils which is likely to be absent from isolated HA fractions.

The rate of Org-^{129}I production was greater in the systems spiked with $^{129}IO_3^-$ than those spiked with $^{129}I^-$ at the same concentration (Fig. 2). However, in mixed systems the *initial* rate of Org-^{129}I production was greater than in solutions spiked with $^{129}IO_3^-$ alone, although a slightly lower concentration of Org-^{129}I was eventually present after 500 hr incubation (e.g. IO_{44} and Mix_{44}). However comparison of systems with the same initial concentration of $^{129}IO_3^-$ (e.g. IO_{22} and Mix $_{44}$) showed that Org-^{129}I concentrations were substantially greater in the mixed systems where $^{129}I^-$ was

also present compared to the equivalent $^{129}IO_3^-$-spiked system. This may suggest that redox coupling between $^{129}I^-$ (or $^{127}I^-$) and $^{129}IO_3^-$ had occurred in the mixed spike solutions (Eq. 2):

$$IO_3^- + 5I^- + 6H^+ \rightleftharpoons 3I_2 + 3\,H_2O \quad (2)$$

When only $^{129}I^-$ was added, its transformation to Org-^{129}I did not depend upon concentration (Fig. 3), suggesting its oxidation mechanism was independent of the presence of another species. However, considering the presence of native iodide ($^{127}I^-$) in the HA solutions, the *relative* rate of $^{129}I^-$ production, from $^{129}IO_3^-$, in the mixed spike system was greater when lower concentrations of $^{129}IO_3^-$ were added (Fig. 3); this result is consistent with faster reduction of IO_3^- (to I^-) at higher iodide/iodate ratios. For the mixed-spike system the ratio of measured iodide to added iodide progressively exceeded 1.0, reflecting the production of I^- from reduction of added IO_3^-.

The *relative* rates of $^{129}IO_3^-$ loss in both $^{129}IO_3^-$- and mixed-spike systems were slightly greater at lower IO_3^- concentrations with similar rates observed for systems with the same total ^{129}I concentration (Fig. 4). Again, this suggests that the rate of iodate reduction is limited, either by the concentration of iodide (Eq. 2) or some other reductive mechanism associated with the HA.

Figure 5 compares the concentrations of species measured in systems where a mix of species was added with the *sum* of species from the appropriate $^{129}I^-$ and $^{129}IO_3^-$ treatments spiked with a single species (e.g. Mix_{44} compared with I_{22}+IO_{22}). Although it could be argued that this comparison is not completely valid because the ^{129}I:HA ratio differed, the rate of $^{129}I^-$ transformation to Org-^{129}I (Fig. 3, open symbols) indicated that HA concentration is not a limiting factor. Figure 5 suggests that initially there was less $^{129}I^-$, and consequently greater concentrations of $^{129}IO_3^-$ and Org-^{129}I, in the mixed spike systems (circles fall below the 1:1 line). However, the difference in species composition between the mixed and single-species systems generally declined with time - eg highest values for iodide (open and closed circles).

Comparison of the concentrations of the species present in single species spiked systems with $^{129}I^-$-spiked systems at an equivalent total iodine concentration (e.g. IO_{44} + I_{44} compared with I_{88}) also show that $^{129}I^-$ was only transformed to Org-^{129}I and that this happened faster when $^{129}IO_3^-$ was present, perhaps reflecting the 5:1 ratio in Eq. 2.

4.2 Iodine distribution within the HA

The distribution of iodine within the HA was examined using SEC-ICP-MS. Lower molecular weight (LMW) HA may be expected to react more easily with iodine due to its greater surface area which may provide greater accessibility to reactive sites. Conversely, the greater negative charge density

expected on LMW fractions may act to exclude or delay I^- or IO_3^- ions from interaction. Xu et al. (2011a), in a study where IO_3^- was added to HA at pH 3, observed that the LMW fractions (3 – 50 kDa) sorbed more iodine than the > 50 kDa fractions after 72 hr. By contrast, Christiansen and Carlsen (1991) observed no dependence on MW size fraction following a rapid (20 min) reaction of Aldrich HA with I^- in the presence of peroxidase enzymes. Figure 6 shows the cumulative integrated counts per second (ICPS) for the organic portion of the SEC chromatogram for added ^{129}I and pre-existing ^{127}I in the HA after a 77 day incubation of the Mix_{88} solution. Higher molecular weight (HMW) molecules elute first due to exclusion from the column matrix - shown by the prominent peak around 400 s. The lines representing the cumulative integrated signals for ^{127}I and ^{129}I in Figure 6 suggest that a greater proportion of ^{127}I than ^{129}I was present in larger HA molecules. Approximately 50% of the cumulative integrated signal for ^{127}I had been detected by 530 s, compared to 600 s for ^{129}I. This indicates that ^{129}I had not fully mixed with the pre-existing HA-bound ^{127}I and had reacted preferentially with the LMW fractions of HA. It also indicates the presence of recalcitrant iodine (^{127}I), unavailable to mix with the added ^{129}I, and with a greater presence in the HMW fractions of HA. Comparison of the Mix_{88} 77 day chromatogram for ^{127}I and ^{129}I (Figure 6) also shows a smaller excluded peak maxima compared to the main organic peak for ^{129}I and a shift in the ^{129}I peak maxima towards LMW fractions, again suggesting preferential binding of freshly added iodine to LMW fractions of HA in contrast to (native) ^{127}I.

4.3 Modelling

Fitted model (Fig. 1) predictions are compared to the observations in Fig. 2 and estimated rate coefficients are given in Table 3. Overall the model fit was good (for all data: $r^2 = 0.96$, $p < 0.001$), supporting the model structure. The values of the (apparent) rate constants broadly reflect the dynamics of the system. Iodate is rapidly converted to humic-bound forms ($k_4 = 2.62\ hr^{-1}$) but the optimal model fit required a reverse reaction ($k_5 = 0.157\ hr^{-1}$) suggesting an approach to an equilibrium position rather than a zero sink for iodate. The further reduction of iodate to iodide was slower ($k_1 = 4.11 \times 10^{-3}\ hr^{-1}$) and both the 'direct' conversion of iodide to humic-bound iodine and the re-mineralisation of iodide were comparatively very slow reactions ($k_3 = 3.16 \times 10^{-4}$ and $k_2 = 4.67 \times 10^{-4}\ hr^{-1}$).

In order to investigate the availability of ^{127}I for mixing with ^{129}I, modelling was extended to 250 d. At this point a pseudo-steady-state was apparent, with no significant changes in species concentrations from 200 d after spiking. After 250 d contact between ^{129}I and HA the model predicted that $^{129}I^-$ /Org-^{129}I = 0.24, whereas the measure ratio $^{127}I^-$ /Org-^{127}I was lower, at 0.17. Therefore although the model prediction suggested that ^{129}I was at equilibrium, a greater proportion of ^{127}I than ^{129}I existed

as Org-I, suggesting the presence of a recalcitrant pool of ^{127}I, unavailable for isotopic mixing. From the $^{129}I^-$ /Org-^{129}I ratio and measured $^{127}I^-$ in solution, the estimated labile Org-^{127}I was 62.9 µg L^{-1}, suggesting that 64% of the HA bound iodine was labile and 36% was incapable of isotopic mixing within 250 d.

Keppler et al. (2003) and Xu et al. (2011b) suggested that iodination of HA occurs early in the humification of fresh plant material with fewer binding sites available as humification progresses. Steric hindrance by aliphatic chains may also make some aromatic binding sites less accessible to freshly added iodine, while effectively 'fixing' native iodine (Xu et al., 2012). Schwehr et al (2009) also observed, in an experiment where natural sediments were spiked with I^-, that recently added I^- was less strongly sorbed than native iodine, and that greater added concentrations resulted in a smaller proportion bound. Therefore although organic-rich soils may well contain higher total concentrations of iodine much of that iodine may not be readily accessible to plants.

5 Conclusions

Inorganic iodine (both I^- and IO_3^-) reacted with HA to produce Org-I. The reaction was slower with I^- compared to systems spiked with IO_3^- or a mixture of IO_3^- and I^-. In mixed and IO_3^--spiked systems I^- concentrations increased rapidly and remained higher than Org-I concentrations throughout the duration of the experiment.

Native iodine in the HA solutions was present only as I^- and Org-I; no IO_3^- was observed. There was evidence that the presence of native $^{127}I^-$ allowed more rapid reduction of spiked $^{129}IO_3^-$, potentially by redox coupling with I^-. This was supported by the relative rates of reaction of the two species, with a faster reaction observed when a mix of inorganic species (I^- and IO_3^-) was added, rather than a single species (I^- or IO_3^- alone). In soils, by contrast, I^- has been reported to transform to Org-I more quickly than IO_3^-, possibly due to the presence of metal oxides or enzymatic oxidation. In a 'purified' HA solution the same reaction mechanisms are not available and I^- oxidation was relatively slow.

Size exclusion chromatography showed that ^{129}I became associated with both high and low molecular weight HA although a slight preference for lower molecular weight fractions was suggested. The native and spiked isotopes were not fully mixed after ~ 2 months of reaction indicating the presence of a recalcitrant pool of ^{127}I; this was also strongly indicated by modelling over longer timescales.

6 Acknowledgements

Funding for H. E. Bowley was provided by UoN and the BGS University Funding Initiative (BUFI-S178).

This work is published with the permission of the Executive Director, British Geological Survey.

7 References

Allard, B. (2006) A comparative study on the chemical composition of humic acids from forest soil, agricultural soil and lignite deposite. Bound lipid, carbohydrate and amino acid distributions. *Geoderma,* **130,** 77 - 96.

Allard, S., von Gunten, U., Sahli, E., Nicolau, R. & Gallard, H. (2009) Oxidation of iodide and iodine on birnessite (d-MnO_2) in the pH range 4-8. *Water Research,* **43,** 3417-3426.

Christiansen, J. V. & Carlsen, L. (1991) Enzymatically controlled iodination reactions in the terrestrial environment. *Radiochimica Acta,* **52-3,** 327-333.

Choung, S., Um, W., Kim, M. & Kim, M-G. 2013. Uptake mechanism for iodine species to black carbon. Environmental Science and Technology 47, 10349 - 10355.

Dai, J. L., Zhang, M., Hu, Q. H., Huang, Y. Z., Wang, R. Q. & Zhu, Y. G. (2009) Adsorption and desorption of iodine by various Chinese soils: II. Iodide and iodate. *Geoderma,* **153,** 130-135.

Dai, J. L., Zhu, Y. G., Huang, Y. Z., Zhang, M. & Song, J. L. (2006) Availability of iodide and iodate to spinach (Spinacia oleracea L.) in relation to total iodine in soil solution. *Plant and Soil,* **289,** 301-308.

Fox, P. M., Davis, J. A. & Luther, G. W. (2009) The kinetics of iodide oxidation by the manganese oxide mineral birnessite. *Geochimica et Cosmochimica Acta,* **73,** 2850-2861.

Francois, R. (1987) The influence of humic substances on the geochemistry of iodine in nearshore and hemipelagic marine sediments. *Geochimica et Cosmochimica Acta,* **51,** 2417 - 2427.

Fuge, R. & Johnson, C. C. (1986) The Geochemistry of Iodine - a Review. *Environmental Geochemistry and Health,* **8,** 31-54.

Gallard, H., Allard, S., Nicolau, R., von Gunten, U. & Croue, J. P. (2009) Formation of iodinated organic compounds by oxidation of iodide-containing waters with manganese dioxide. *Environmental Science & Technology,* **43,** 7003-7009.

Garcia-Suarez, A. M. & Butler, C. J. (2006) Soil temperatures at Armagh Observatory, Northern Ireland, from 1904 to 2002. *International Journal of Climatology,* **26,** 1075-1089.

Hansen, V., Roos, P., Aldahan, A., Hou, X. & Possnert, G. (2011) Partition of iodine (^{129}I and ^{127}I) isotopes in soils and marine sediments. *Journal of Environmental Radioactivity,* **102,** 1096-1104.

Johnson C. C. (2003a) The geochemistry of iodine and its application to environmental strategies for reducing the risks from iodine deficiency disorders (idd). Brit. Geol. Surv., DFID kar project R7411, Report CR/03/057N.

Johnson, C. C. (2003b) Database of the iodine content of soils populated with data from published literature. British Geological Survey Commissioned Report.

310 Keppler, F., Biester, H., Putschew, A., Silk, P. J., Scholer, H. F. & Muller, G. (2003) Organoiodine
311 formation during humification in peatlands. *Environmental Chemistry Letters,* **1,** 219-223.

312 Marshall, S.J. (1992) The complexation of aluminium by humic acids in fresh waters. PhD Thesis.
313 Agricultural and Environmnetal Sciences, University of Nottingham.

314 Marshall, S. J., Young, S. D. & Gregson, K. (1995) Humic acid-proton equilibria: A comparison of two
315 models and assessment of titration error. *European Journal of Soil Science,* **46,** 471-480.

316 Muramatsu, Y. & Wedepohl, K. H. (1998) The distribution of iodine in the Earth's crust. *Chemical*
317 *Geology,* **147,** 201-216.

318 Press , W.H., Teukolsky S.A., Vetterling, W.T., Flannery, B.P. (2007) Numerical Recipes 3rd Edition:
319 The Art of Scientific Computing, Cambridge University Press, New York, NY

320 Reiller, P., Mercier-BIon, F., Gimenez, N., Barre, N. & Miserque, F. (2006) Iodination of humic acid
321 samples from different origins. *Radiochimica Acta,* **94,** 739-745.

322 Saunders, R.W., Kumar, R., MacDonald, S.M. and Plane J.M.C. (2012). Insights into the
323 Photochemical Transformation of Iodine in Aqueous Systems: Humic Acid Photosensitized
324 Reduction of Iodate. Environ. Sci. Technol., **46**, 11854−11861.

325 Schlegel, M. L., Reiller, P., Mercier-Bion, F., Barre, N. & Moulin, V. (2006) Molecular environment of
326 iodine in naturally iodinated humic substances: Insight from X-ray absorption spectroscopy.
327 *Geochimica et Cosmochimica Acta,* **70,** 5536 - 5551.

328 Schwehr, K. A., Santschi, P. H., Kaplan, D. I., Yeager, C. M. & Brinkmeyer, R. (2009) Organo-iodine
329 formation in soils and aquifer sediments at ambient concentrations. *Environmental Science*
330 *& Technology,* 43**,** 7258-7264.

331 Shetaya, W. H., Young, S. D., Watts, M. J., Ander, E. L. & Bailey, E. H. (2012) Iodine dynamics in soils.
332 *Geochimica et Cosmochimica Acta,* **77,** 457-473.

333 Smyth, D. & Johnson, C. C. (2011) Distribution of iodine in soils of Northern Ireland. *Geochemistry-*
334 *Exploration Environment Analysis,* **11,** 25-39.

335 D Tarsitano, D, Young, S.D., Crout, N.M.J. (2011) Evaluating and reducing a model of radiocaesium
336 soil-plant uptake. Journal of Environmental Radioactivity, **102**, 262-269.

337 Warner, J. A., Casey, W. H. & Dahlgren, R. A. (2000) Interaction kinetics of $I_{2(aq)}$ with substituted
338 phenols and humic substances. *Environmental Science & Technology,* **34,** 3180-3185.

339 Weng, H. X., Weng, J. K., Yan, A. L., Hong, C. L., Yong, W. B. & Qin, Y. C. (2008) Increment of iodine
340 content in vegetable plants by applying iodized fertilizer and the residual characteristics of
341 iodine in soil. *Biological Trace Element Research,* **123,** 218-228.

342 Whitehead, D. C. (1974) The infl uence of organic matter, chalk and sequisoxides on the solubility of
343 iodide, elemental iodine and iodate inclubated with soil. *Journal of Soil Science*, **25**, 461-470.

344 Whitehead, D. C. (1984) The Distribution and Transformations of Iodine in the Environment.
345 *Environment International,* **10,** 321-339.

346 WHO (2004) In Iodine Status Worldwide (eds. B. Benoist, et al.). Department of Nutrition for Health
347 and Development, World Health Organization, Geneva.

348 WHO (2008) WHO expert consultation on salt as a vehicle for fortification, Luxembourg, 21-22
349 March 2007. ISBN 978 92 4 159678 7.

350 Xu, C., Miller, E. J., Zhang, S., Li, H.-P., Ho, Y.-F., Schwehr, K. A., Kaplan, D. I., Otosaka, S., Roberts, K.
351 A., Brinkmeyer, R., Yeager, C. M. & Santschi, P. H. (2011a) Sequestration and remobilization
352 of radioiodine (^{129}I) by soil organic matter and possible consequences of the remedial action
353 at Savannah River site. *Environmental Science & Technology,* **45,** 9975-9983.

354 Xu, C., Zhang, S. J., Ho, Y. F., Miller, E. J., Roberts, K. A., Li, H. P., Schwehr, K. A., Otosaka, S., Kaplan,
355 D. I., Brinkmeyer, R., Yeager, C. M. & Santschi, P. H. (2011b) Is soil natural organic matter a
356 sink or source for mobile radioiodine (^{129}I) at the Savannah River Site? *Geochimica et*
357 *Cosmochimica Acta,* **75,** 5716-5735.

358 Xu, C., Zhong, J., Hatcher, P. G., Zhang, S., Li, H.-P., Ho, Y.-F., Schwehr, K. A., Kaplan, D. I., Roberts, K.
359 A., Brinkmeyer, R., Yeager, C. M. & Santschi, P. H. (2012) Molecular environment of stable
360 iodine and radioiodine (I-129) in natural organic matter: Evidence inferred from NMR and
361 binding experiments at environmentally relevant concentrations. *Geochimica et*
362 *Cosmochimica Acta,* **97,** 166-182.

363 Yamada, H., HisamorI, I. & Yonebayashi, K. (2002) Identification of organically bound iodine in soil
364 humic substances by size exclusion chromatography/inductively coupled plasma mass
365 spectrometry (SEC/ICP-MS). *Soil Science and Plant Nutrition,* **48,** 379-385.

366 YamaguchI, N., Nakano, M., Takamatsu, R. & Tanida, H. (2010) Inorganic iodine incorporation into
367 soil organic matter: evidence from iodine K-edge X-ray absorption near-edge structure.
368 *Journal of Environmental Radioactivity,* **101,** 451-457.

369 Yntema, L. F. & Fleming, T. (1939) Volumetric oxidation of iodide to iodate by sodium chlorite.
370 *Industrial and Engineering Chemistry-Analytical Edition,* **11,** 0375-0377.

371

Tables

Table 1: Summary of added iodine (^{129}I) species in incubated HA solutions.

Table 2: Measured characteristics of a humic acid (HA) isolated from the Ah horizon of a coniferous plantation soil in Leicestershire (UK); (52^{o} 42' N, 1^{o} 14' W; 195 m).

Table 3: Optimised parameter values (first-order rate constants) describing HA-iodine dynamics in the model shown in Figure 1.

Table 1: Summary of added iodine (^{129}I) species in incubated HA solutions.

Solution	$^{129}I^-$ added ($\mu g\ ^{129}I\ L^{-1}$)	$^{129}IO_3^-$ added ($\mu g\ ^{129}I\ L^{-1}$)
I_{22}	22.1	0
I_{44}	44.1	0
I_{88}	88.2	0
IO_{22}	0	22.1
IO_{44}	0	44.1
IO_{88}	0	88.2
Mix_{22}	11.0	11.0
Mix_{44}	22.1	22.1
Mix_{88}	44.1	44.1

Table 2: Measured characteristics of a humic acid (HA) isolated from the Ah horizon of a coniferous plantation soil in Leicestershire (UK); (52° 42' N, 1° 14' W; 195 m).

Characteristic	Value	Units	Source
Ash content	0.66*	%	Marshall (1992)
Total acidity	6.49*	$mol_c\ kg^{-1}$	Marshall (1992)
Dissolved organic carbon	3.67	$mg\ ml^{-1}$	DOC analysis
^{127}Iodide#	15.1	$\mu g\ I\ L^{-1}$	SEC analysis
Org-^{127}I#	98.0	$\mu g\ I\ L^{-1}$	SEC analysis

*Ash content and total acidity are the mean of two measurements quoted by Marshall (1992).
Measured in HA suspensions

Table 3: Optimised parameter values (first-order rate constants) describing HA-iodine dynamics in the model shown in Figure 1.

Rate constant	Mean (hr^{-1})	S. D.
k1	0.00411	0.00010
k2	0.000467	0.00004
k3	0.000316	0.00002
k4	2.62	0.00000
k5	0.157	0.00003

Figures

Figure 1: Conceptual model describing transformations of spiked ^{129}I in the presence of HA. Rate constants k_1–k_5 describe first-order rate equations.

Figure 2: Modelled (lines) and measured (symbols) change in ^{129}I concentrations with time following spiking with ^{129}I at a range of concentrations and species compositions. Species measured included $^{129}I^-$ (black circles ●, black lines), $^{129}IO_3^-$ (open squares □, dashed lines) and Org-^{129}I (grey triangles▲, grey lines). Error bars show standard error of triplicate measurements.

Figure 3: Change in the ratio of measured iodide to added iodide over time, following addition of iodide (*open* symbols) and mixed iodide/iodate ^{129}I spikes (*closed* symbols). Total concentrations of ^{129}I added were: 22.1 µg L^{-1} (circles), 44.1 µg L^{-1} (squares) and 88.2 µg L^{-1} (triangles).

Figure 4: Change in ratio of measured iodate to added iodate over time, following addition of iodate (*open* symbols) and mixed iodide/iodate ^{129}I spikes (*closed* symbols). Total concentrations of ^{129}I added were: 22.1 µg L^{-1} (circles), 44.1 µg L^{-1} (squares) and 88.2 µg L^{-1} (triangles).

Figure 5: Comparison of total concentrations of iodine-129 species in solution in mixed and single spiked systems at total iodine concentrations of 44 µg L^{-1} (*open* symbols) and 88 µg L^{-1} (*closed* symbols). Dashed line = 1:1, square symbols = iodate, circles = iodide, triangles = Org-I.

Figure 6: Cumulative ICPS (integrated counts per second) as a percentage of total counts, from size exclusion chromatograph of ^{129}I (thick black line) and ^{127}I (thick grey line); 25%, 50% and 75 % of cumulated ICPS are indicated by circles, squares and diamonds, respectively. The Org-I section of ^{127}I (thin black line) and ^{129}I (thin grey line) SEC chromatograms (2^o Y-axis) are also shown. All data are for the Mix_{88} solution (Table 1) after 77 days incubation.

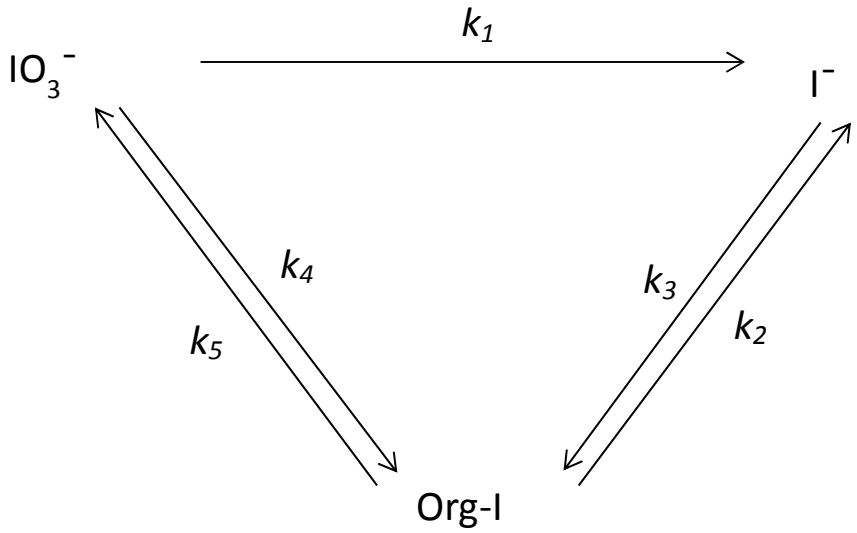

Figure 1: Conceptual model describing transformations of spiked ^{129}I in the presence of HA. Rate constants k_1–k_5 describe first-order rate equations.

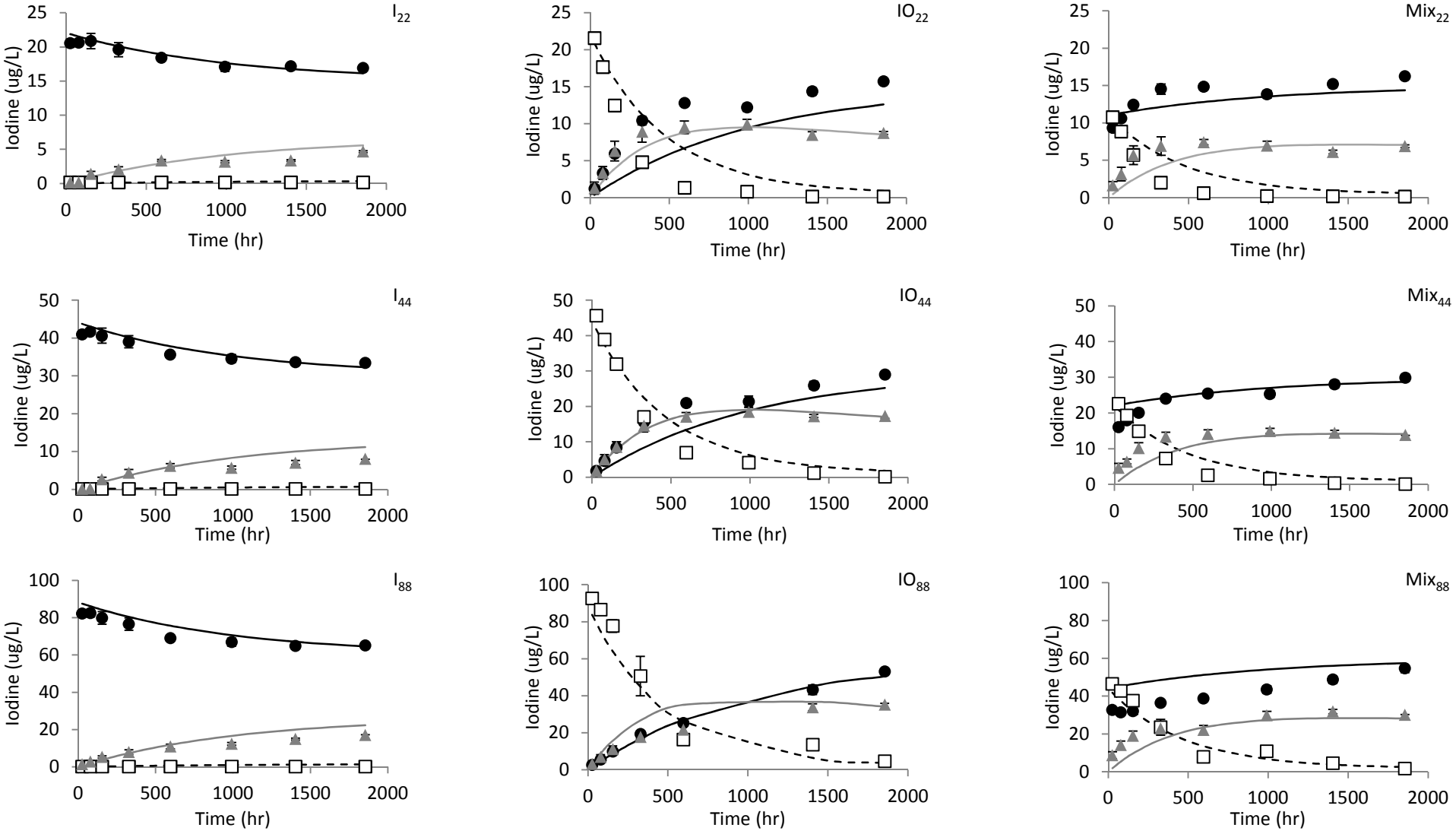

Figure 2: Modelled (lines) and measured (symbols) change in ^{129}I concentrations with time following spiking with ^{129}I at a range of concentrations and species compositions. Species measured included $^{129}I^-$ (black circles ●, black lines), $^{129}IO_3^-$ (open squares □, dashed lines) and Org-^{129}I (grey triangles ▲, grey lines). Error bars show standard error of triplicate measurements.

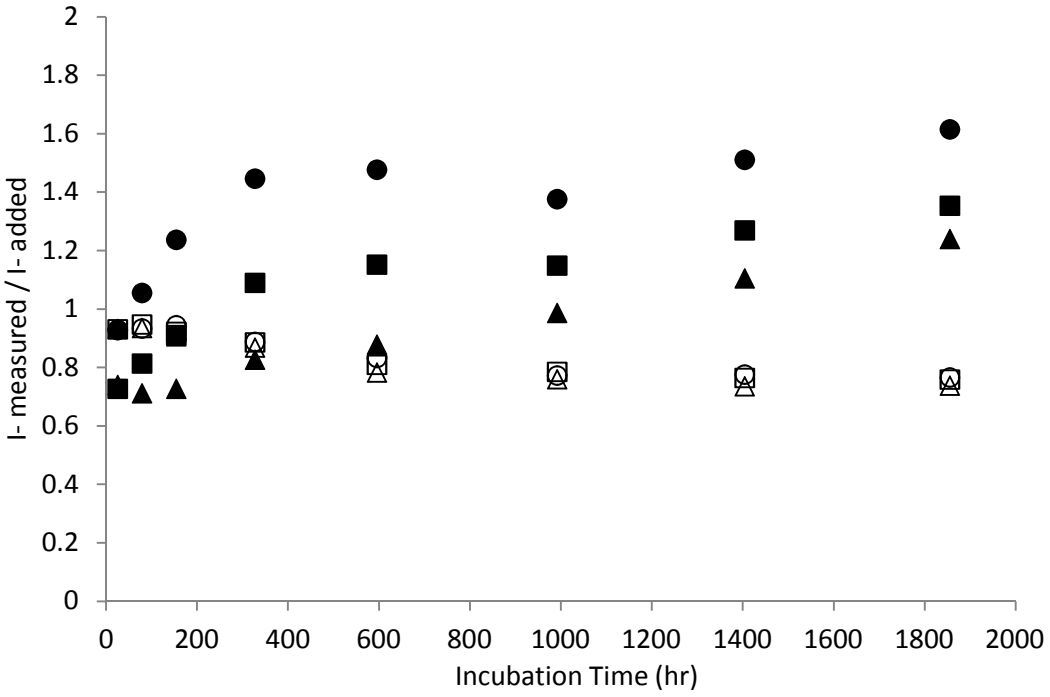

Figure 3: Change in the ratio of measured iodide to added iodide over time, following addition of iodide (*open* symbols) and mixed iodide/iodate ^{129}I spikes (*closed* symbols). Total concentrations of ^{129}I added were: 22.1 µg L^{-1} (circles), 44.1 µg L^{-1} (squares) and 88.2 µg L^{-1} (triangles).

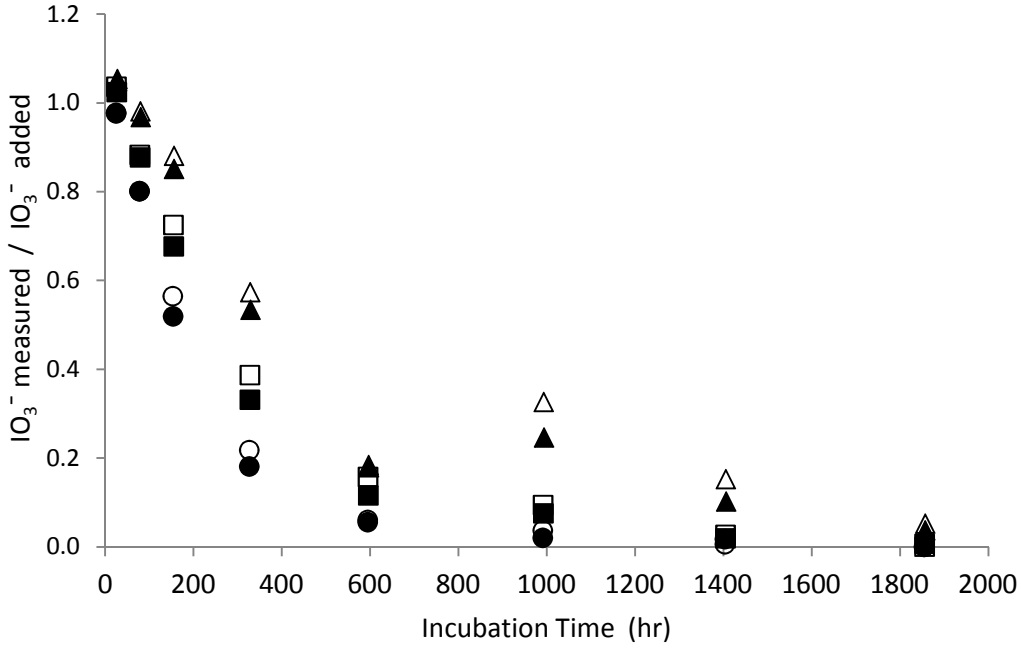

Figure 4: Change in ratio of measured iodate to added iodate over time, following addition of iodate (*open* symbols) and mixed iodide/iodate ^{129}I spikes (*closed* symbols). Total concentrations of ^{129}I added were: 22.1 µg L^{-1} (circles), 44.1 µg L^{-1} (squares) and 88.2 µg L^{-1} (triangles).

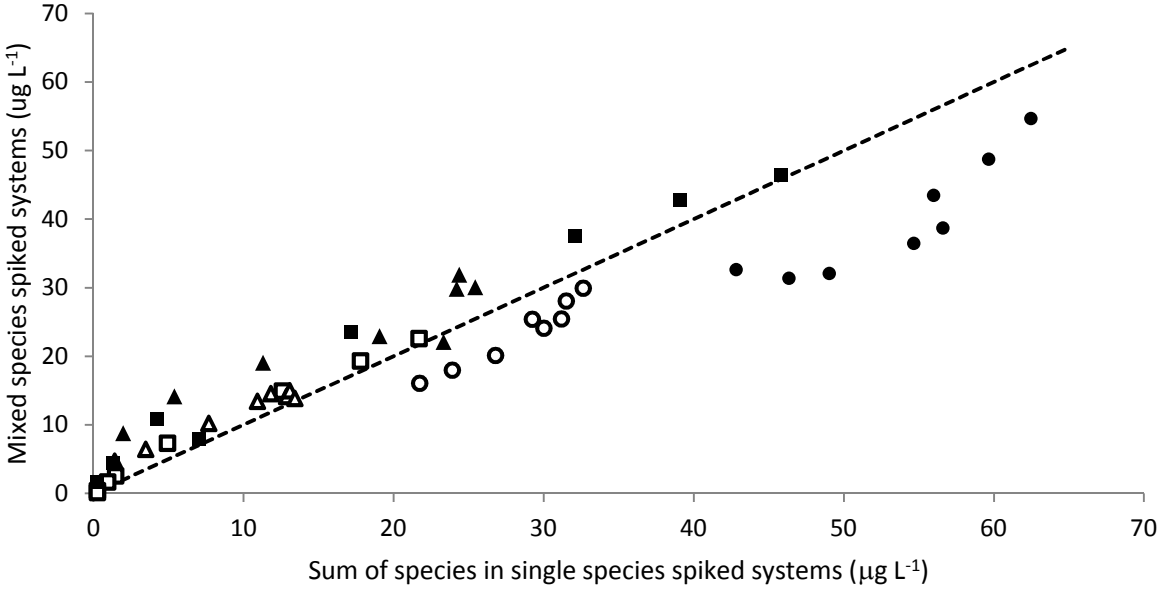

Figure 5: Comparison of total concentrations of iodine-129 species in solution in mixed and single spiked systems at total iodine concentrations of 44 µg L^{-1} (*open* symbols) and 88 µg L^{-1} (*closed* symbols). Dashed line = 1:1 relationship, square symbols = iodate, circles = iodide, triangles = Org-I.

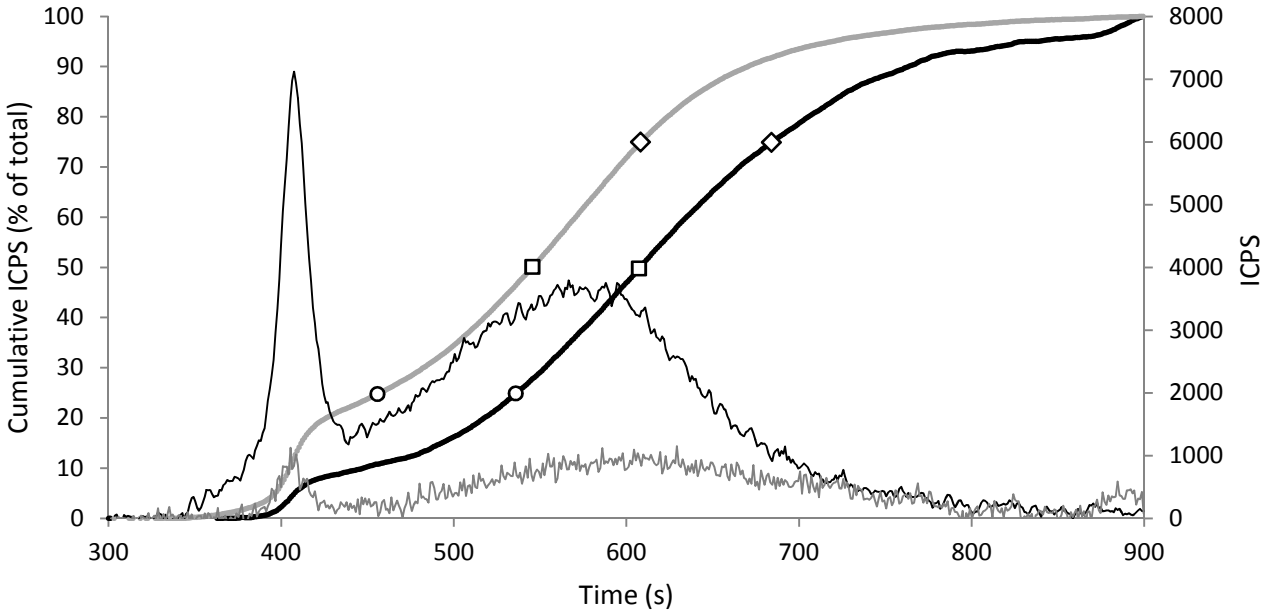

Figure 6: Cumulative ICPS (integrated counts per second) as a percentage of total integrated counts, from size exclusion chromatograph of ^{129}I (thick black line) and ^{127}I (thick grey line); 25%, 50% and 75 % of cumulated ICPS are indicated by circles, squares and diamonds, respectively. The Org-I section of ^{127}I (thin black line) and ^{129}I (thin grey line) SEC chromatograms (2^{o} Y-axis) are also shown. All data are for the Mix_{88} solution (Table 1) after 77 days incubation.

Electronic Annex A: Correction applied for the presence of ^{127}I in the ^{129}I SRM 4949C:

All measured ^{129}I concentrations had a correction applied to nominally ascribe *all* iodine added in ^{129}I spikes (^{129}I + ^{127}I) to ^{129}I, for ease of description:

$$^{129}\mathrm{I} = {}^{129}\mathrm{I}_{\mathrm{meas}} \times 1.12 \times (127/129) \qquad \text{(A1)}$$

Where ^{129}I = 'corrected' concentration of I from the spike in solution (µg L^{-1}) i.e. (^{129}I + ^{127}I present in the spike), $^{129}I_{meas}$ = measured concentration of ^{129}I (µg L^{-1}), 1.12 corrects for the presence of 12 % ^{127}I in the ^{129}I and (127/129) is a gravimetric correction. The corresponding correction was also applied to measurements of ^{127}I, according to Eqn. A2:

$$^{127}\mathrm{I} = {}^{127}\mathrm{I}_{\mathrm{meas}} - \left(0.12 \times {}^{129}\mathrm{I}_{\mathrm{m}}\right) \qquad \text{(A2)}$$

Where ^{127}I = 'corrected' concentration of ^{127}I in solution (µg L^{-1}) i.e. ^{127}I minus the ^{127}I present as a result of the spiking, and $^{127}I_{meas}$ = measured concentration of ^{127}I (µg L^{-1}).